Journal of Biosciences and Medicines, 2025, 13(8), 146-157
https://www.scirp.org/journal/jbm
ISSN Online: 2327-509X
ISSN Print: 2327-5081

# Computational Insights into Moxifloxacin Resistance Conferred in Asn499 Mutants of *Mycobacterium tuberculosis* DNA Gyrase

**MunMyong Choe[1*], ChungIl Ri[1], ChunHyok Ku[1], JiUng Hwang[1], SangIk Pak[1], Qian Lu[2*]**

[1]R&D Center, Pyongyang University of Science and Technology (PUST), Pyongyang, Democratic People's Republic of Korea
[2]School of Grain Science and Technology, Jiangsu University of Science and Technology, Zhenjiang, China
Email: *MunMyongChoe@163.com, *luqian@just.edu.cn

**How to cite this paper:** Choe, M., Ri, C., Ku, C., Hwang, J., Pak, S. and Lu, Q. (2025) Computational Insights into Moxifloxacin Resistance Conferred in Asn499 Mutants of *Mycobacterium tuberculosis* DNA Gyrase. *Journal of Biosciences and Medicines*, **13**, 146-157.
https://doi.org/10.4236/jbm.2025.138013

**Received:** June 9, 2025
**Accepted:** August 12, 2025
**Published:** August 15, 2025



## Abstract

The mycobacterial enzyme gyrase is the target of second-line tuberculosis (TB) drugs, fluoroquinolones. Emerging mutations in DNA gyrase subunit B including Asparagine (Asn)499Aspartic acid (Asp) and Asn499Lysine (Lys) cause resistance to fluoroquinolones like moxifloxacin (MFX). In this study, we attempted to discover the moxifloxacin resistance using *in silico* techniques such as molecular docking and molecular dynamics simulation. 10 ns of molecular dynamic simulation of gyrase-DNA-Moxifloxacin complex was performed with GROMACS and root mean square deviation (RMSD), root mean square fluctuation (RMSF), radius of gyration (Rg) were calculated to examine the influence of mutation on the stability of the complex. Structural analysis showed that the stability of cleaved complex of wild type was well kept during simulation, while mutant complexes showed unstable states through the calculation of RMSD and Rg. Also, the distance between Tyrosine (Tyr)129, amino acid crucial for function of gyrase, and DNA phosphate in mutant complexes were extended compared with wild type. Binding free energy of moxifloxacin calculated using molecular docking and Molecular Mechanics/Poisson-Boltzmann surface area (MM-PBSA) methods showed the remarkable decreases in the mutant systems comparing with wild one. This study will make contribution to designing of new fluoroquinolones for controlling of drug-resistant tuberculosis.

## Keywords

Molecular Dynamics Simulation, Molecular Docking, DNA Gyrase, *Mycobacterium tuberculosis*, Fluoroquinolone

## 1. Introduction

Tuberculosis is an infectious disease caused by pathogenic bacteria *Mycobacterium tuberculosis* and became one of the 10 lethal diseases in the world [1]. Fluoroquinolones are the second line anti-tuberculosis drugs [2] and shorten the treatment period of disease [3]. These broad-spectrum antibiotics exert their activity by inhibiting mycobacterial enzyme DNA gyrase [4]. DNA gyrase constitutes hetero-tetramer consisting of two subunits, GyrA and GyrB (GyrA2GyrB2), and N-terminal domain of GyrA and Toprim domain of GyrB form the reaction core [5]. Negative supercoiling introduced by the DNA gyrase facilitates the DNA unwinding which stimulates DNA replication and transcription. The residues of GyrA are involved in breakage-reunion process whereas adenosine triphosphate (ATP) hydrolysis is performed by GyrB subunit [6].

Many drug-resistant tuberculosis strains are emerging throughout the world and this makes the treatment of tuberculosis with current antibiotics including fluoroquinolones more difficult. The fluoroquinolone-resistance is mostly related to the mutation of gyrase gene, and most common resistant mutations are at gyrA and mutations in gyrB also cause high resistance to fluoroquinolones like ofloxacin and moxifloxacin (MFX) [7].

Recently, the crystal structures of TB gyrase-fluoroquinolone cleaved complexes constituting GyrA, GyrB, DNA oligonucleotides, magnesium (Mg) ion and fluoroquinolones were determined [8]. Subunit A consists of a N-terminal breakage-reunion domain and a carboxy-terminal domain and subunit B consists of ATPase domain and Toprim domain. Importantly, the breakage-reunion domain and the Toprim domain, two domains from different subunits, form the enzyme reaction core. The fluoroquinolones targeting gyrase bind to the enzyme-DNA complex, stabilizing this complex and resulting in the blocking of DNA replication [9].

Several point mutations in the GyrB including Asp500Asn, Asn499Asp and Asn499Lys and its genetic background were reported in many studies [10]-[12]. Among these mutations, Asn499Asp mutation cause cross-resistance to four fluoroquinolones involving ciprofloxacin, levofloxacin, ofloxacin and moxifloxacin while Asn499Lys mutation conferred resistance moxifloxacin only [13]. Especially, Asn499Asp mutation was also associated with fourfold increases in resistance to quinolones and 12 - 30 fold decrease in DNA supercoiling activity inhibition in some isolates [10]. Clinical isolates and transductants harboring Asn499Asp mutation conferred resistance to all fluoroquinolones and their minimum inhibition concentrations (MICs) were at least 4 fold bigger than wild isolates [13]. Fluoroquinolone-resistance mechanism of mutation at the Asn499 residue of GyrB was not fully illuminated despite these mutations play a crucial role in resistance. To analyze the impacts of these mutations on the moxifloxacin efficacy in the dynamic behavior, molecular dynamics (MD) simulation was conducted with gyrase-DNA-MFX complex. Also, the molecular docking give helps to the understanding of drug-resistance mechanism. Mutation of Asn499 residue makes the

structure of gyrase-DNA complex unstable and decreases the binding energy of moxifloxacin in mutant structures comparing with wild one.

## 2. Materials and Methods

### 2.1. Preparation of Gyrase Structures

The crystal structure of the gyrase reaction core used in this study was retrieved from protein data bank (https://www.rcsb.org) (PDB ID: 5BS8). This structure contains breakage-reunion domain of GyrA and Toprim domain of GyrB and moxifloxacin as a ligand as well as DNA oligonucleotides and Mg ion. As mutant structures were not provided, *in-silico* mutation was done by mutating Asn499 to Asp and Lys using DS 2017 (Discovery Studio 2017 R2, BIOVIA Corp. San Diego, USA). The 3D structure of moxifloxacin was downloaded from Drugbank database (ID: DB00218) in sdf format. Gyrase-DNA-ligand complexes of wild and mutant structures were projected to 10ns MD simulation.

### 2.2. Molecular Dynamics Simulation

MD simulation was performed using GROMACS 2019 software package [14] in GROMOS 54A6 force field [15]. DNA and ligand topology for MD simulation were prepared by PRODRG server [16]. Gyrase-DNA-ligand complex was solvated in a cubic box with simple point charge (SPC) water model. Sodium ions were added for neutralization of the system. Then the system was energy-minimized by steepest descent algorithm. It was equilibrated by NVT ensemble (Constant number of particles, Volume, Temperature) for 100 ps. Berendsen thermostat algorithm was applied for temperature coupling at 310 K [17]. The system was also equilibrated in NPT (Constant number of particles, Pressure, Temperature) condition for 100 ps using Parrinello-Rahman method [18]. Particle Mesh Ewald method [19] was used for long-range electrostatics using cut-off length of 0.9 nm and linear constraint solver (LINCS) method [20] was employed to constrain the system. Simulation was done for 10 ns and trajectories were recorded at every 1000 steps for analysis. GROMACS-inbuilt tools were used to calculate the root mean square deviation (RMSD), root mean square fluctuation (RMSF) and radius of gyration (Rg) by analyzing the structural changes. In general, bigger RMSD and RMSF values show instability compared with smaller one and in our study the frequency was observed to assess and compare the dynamic stability of the gyrase-ligand complexes and evaluate the dynamic tendency. The distances between some amino acid residues in the MFX binding site was analyzed to observe the conformational change of the ligand binding site.

### 2.3. Molecular Docking Analysis and MM-PBSA Binding Energy Calculation

AutoDock 4.2 [21] was used to perform molecular docking analysis. The grid point spacing was set to 0.375 Å. Docking was performed with 150 runs of the Lamarckian genetic algorithm (LGA), using a maximum of $25 \times 10^6$ energy eval-

uations, a maximum number of $27 \times 10^3$ generations, a gene mutation rate of 0.02 and a crossover rate of 0.8 [21] [22].

In this study, the binding free energies were calculated with g_mmpbsa package using the Molecular Mechanics/Poisson-Boltzmann surface area (MM-PBSA) algorithm [23]. 21 snapshots were chosen by every 0.5 ns from MD trajectory. The binding energy consists of three energetic terms, potential energy in vacuum, polar-solvation energy and non-polar solvation energy. The vacuum, solvent and solute dielectric constants were set at 1, 80 and 2, respectively. The calculation of nonpolar solvation energy was based on solvent accessible surface area (SASA) model. The entropy contribution was not included in the calculation of binding energy.

## 3. Result and Discussion

### 3.1. The Structural Stability of the Cleaved Complex

One of the important measures to compare the inhibitive activities of gyrase-inhibiting drugs is the stability of gyrase-DNA-fluoroquinolone cleaved complex [8]. Although mutations in gyrB are rarely emerged but recent studies found that the impact of gyrB mutations was obvious on fluoroquinolone resistance [24]. Mutation of Asn499 of GyrB lowered the inhibitive activity of MFX, resulting in recovery of gyrase activity. The activity of enzyme is mostly related to its structure and the structural change of enzyme leads to the its change of activity.

MD simulation showed that the structure of cleaved complex kept its stability in wild typed system while mutated systems had tendency of instable states (**Figure 1**).

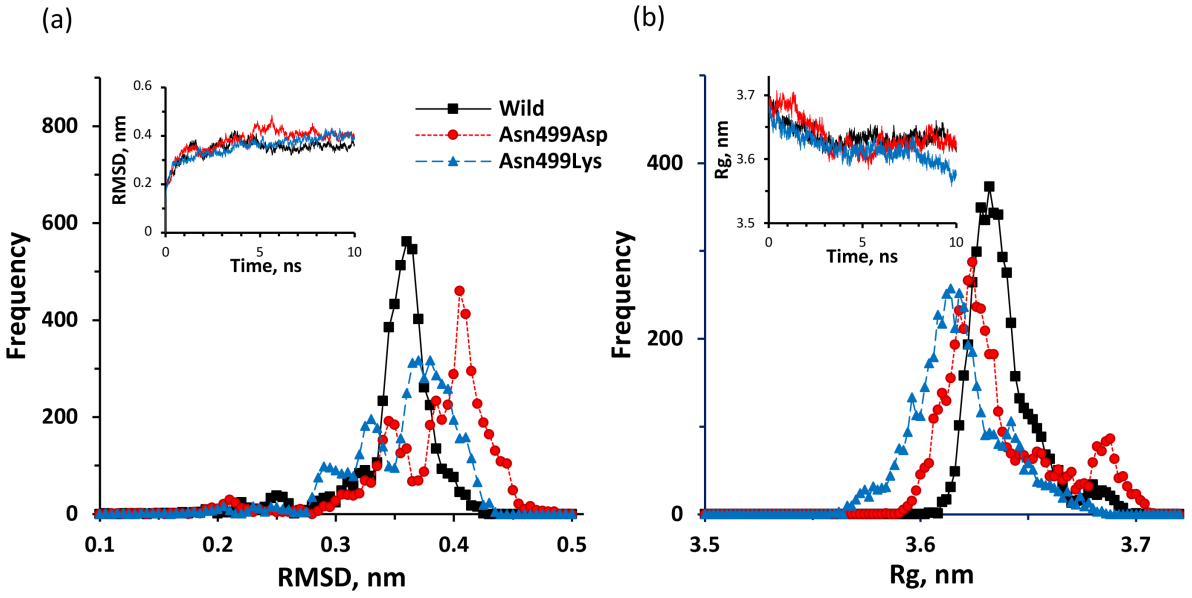


**Figure 1.** Graphs showing RMSD (a) and Rg values (b) of cleaved complex during simulation. Time-dependent plot placed in the distribution plot. Wild type is colored in black, Asn499Asp mutant is colored in red and Asn499Lys is colored in blue.

In detail, RMSD distribution in wild system made a single peak at ~0.3 nm (frequency = ~600), meaning that maintained equilibrium in RMSD values for entire time. However, in Asn499Asp and Asn499Lys systems, 2 and 3 peaks in RMSD distribution were observed, respectively. These RMSD distributions in cleaved complexes referred that wild system had more stable dynamic features than mutant systems.

Also, Rg distribution of cleaved complex showed the comparison between wild and mutant systems. Rg value is an index for measuring the compactness of structure so it is necessary to analyze the Rg values of cleaved complex for estimating its structural stability. Wild cleaved complex had the one peak of the highest frequency at ~370 in Rg distribution, relating the approximately unchanged tendency of Rg values. In comparison, in Asn499Asp cleaved complex, Rg distribution had 2 peaks with frequencies with less than 300 because Rg values for the first 3 ns decreased sharply from ~3.7 nm to ~3.6 nm and then kept Rg values for rest of time. Then, Asn499Lys system showed the one peak of Rg distribution with ~260 of frequency value due to the continuous decrease of Rg values for entire simulation time. RMSD and Rg distributions totally suggested that wild cleaved complex had more stable dynamic tendency than Asn499Asp and Asn499Lys systems.

### 3.2. The Flexibility and Structural Change of MFX Binding Cavity

MFX binds the space between the gyrase and DNA strand (Figure 2) and the structural stability of MFX binding cavity significantly influences the binding of drug.

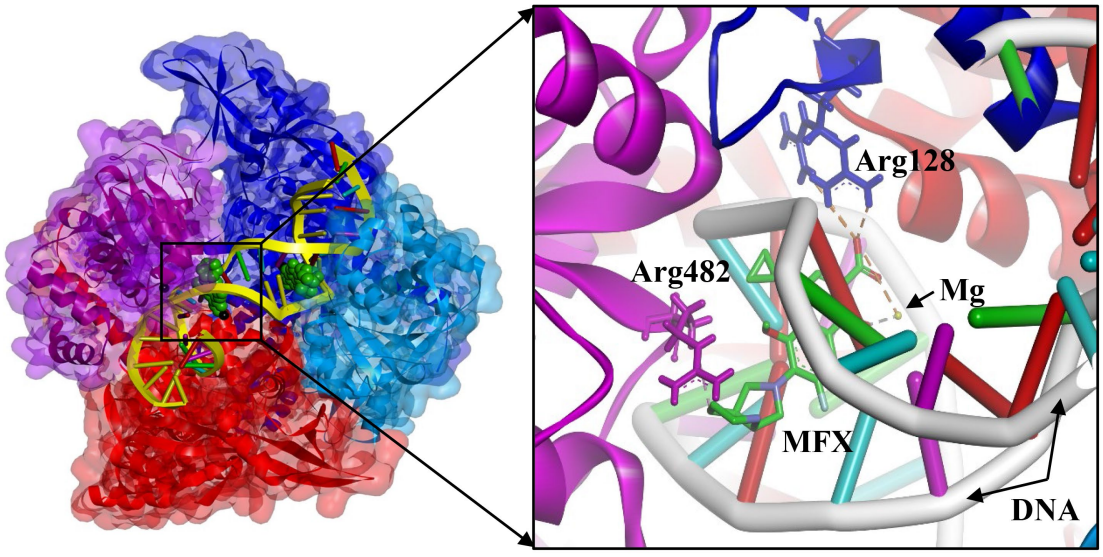


Figure 2. The structure of gyrase-DNA-MFX complex and MFX binding site.

As shown in Figure 2, in wild structure MFX interacted with Arg482 of GyrB and Arg128 of GyrA as well as Mg ion and DNA molecule. Asn499 residue do not interact with MFX even though Asn499 is located in the surrounding of MFX.

MFX binding cavity consists of gyrase residues, DNA strand and Mg ion but the determinant is conformational change of binding pocket because the residual and structural change of residues in MFX binding cavity can directly affect the stability of MFX binding. MD simulation showed the alteration of residual flexibility in the different systems through RMSF values (Figure 3).

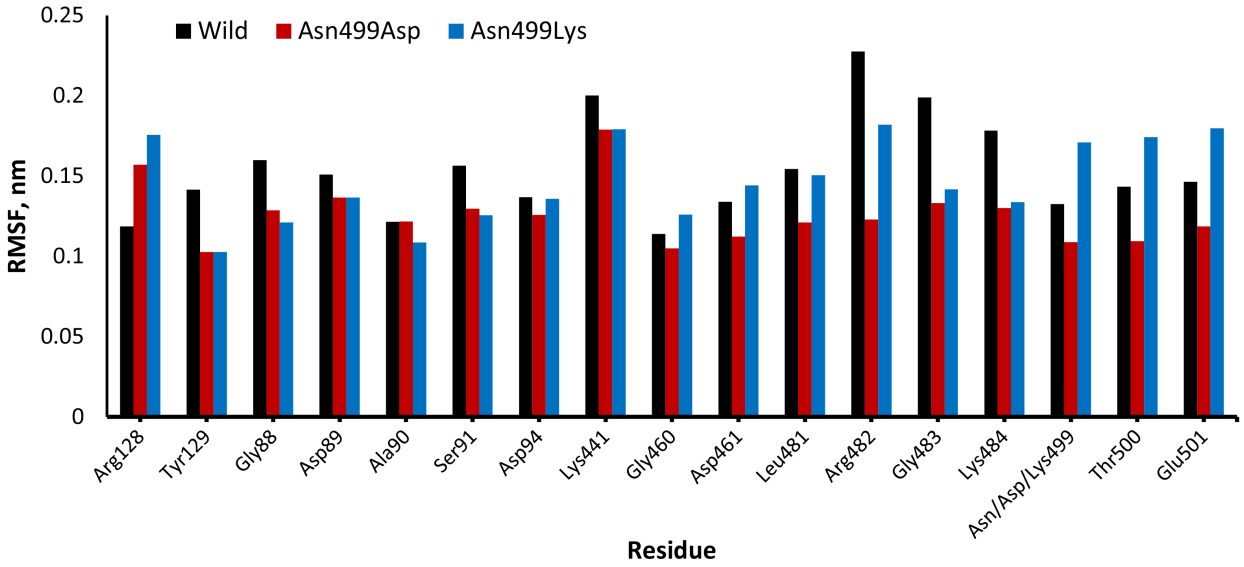


Figure 3. Bar chart of RMSF of MBS residues in wild and mutant gyrase structures. Black color represents for wild type, red color for Asn499Asp and blue color for Asn499Lys mutants.

MFX surroundings within 0.6 nm distance were 17 amino acids including Arg482, Arg123 and Asn499, and RMSF values of these residues reflected the structural change features of MFX binding cavity.

RMSF values of Asp94, Asp89 and Ala90 of GyrA were not changed in wild and mutant gyrases, while Arg128 residue in wild structure had smaller RMSF value than those in both mutant structures and Tyr129, Gly88, Ser91, Lys441, Gly483 and Lys484 residues acted inversely. Also, RMSF values of Gly460, Asp461, Leu481 and Arg482 of GyrB in Asn499Asp mutant were smallest among wild and Asn499Lys mutant, of which their RMSF values were approximately equal or slightly different, while RMSF values of Asn499, Thr500 and Glu501 residues were ordered at Asn499Lys > Wild > Asn499Asp. MFX binding cavity residues of GyrA except Arg128 had similar trends of which RMSF values in wild structure were greater than mutants and residues of GyrB except Lys441 had trend of having smallest RMSF in Asn499Asp. Obviously, the residue of interest, Asn499, had change in flexibility and also other residues' flexibility had changed respectively, in spite of different ordered RMSF in different systems. Therefore, the alteration of residual flexibility of MFX binding site may change the binding stability of MFX by structural change of molecular binding site (MBS).

Also, through the calculation of distances between MBS residues, the structural change of MBS in mutant gyrases was evaluated.

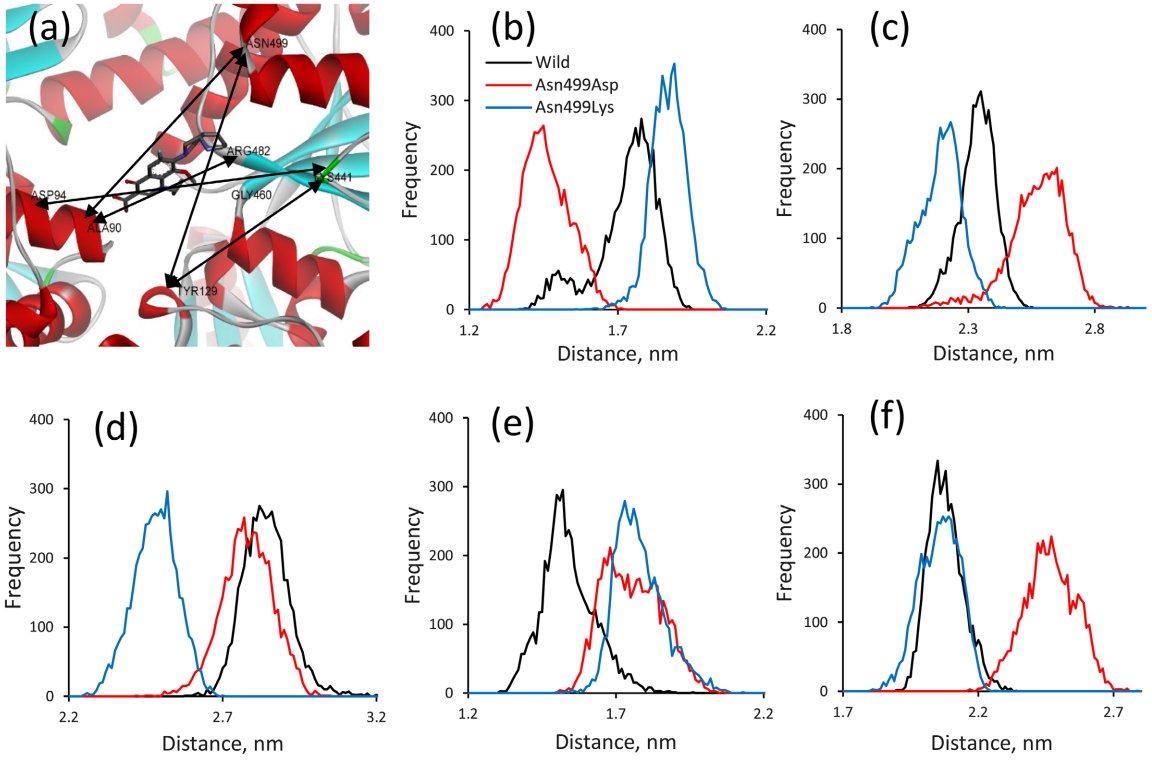


**Figure 4.** The distance between residues of MFX binding site (a) residues around MFX (b) Ala90-Arg482, (c) Ala90-Asn499, (d) Asp94-Lys441, (e) Tyr129-Lys441, (f) Tyr129-Asn499.

As shown in **Figure 4**, the distances between MBS residues were changed in mutant systems compared to wild system. The distance between Ala90 and Arg482 showed contraction in Asn499Asp mutants, while wild and Asn499Lys mutant were almost kept in similar distance. On the other hand, in Asn499Asp mutant expanded the distance between Ala90 and Asn499 residues and between Tyr129 and Asn499. Then, the distance between Tyr129 and Lys441 expanded in both mutant systems and Asp94 had decreased distance from Lys441 in Asn499Lys mutant.

The distance changes between MBS residues during simulation showed the obvious structural change of MBS and these changes may affect the interaction of MFX and its surroundings.

### 3.3. Interaction of MFX and MBS Residues

MFX can bind to the gyrase firmly to inhibit the activity of enzyme and the MFX resistance of mutant gyrase may be correlated to the unstable interaction between MFX and its binding site.

Molecular docking result showed the difference in MFX interaction in wild and mutant gyrases, well correlated to previous research [25].

The binding energy of MFX to MBS calculated by AutoDock 4.2 were −9.9 kcal/mol in wild gyrase and −9.61 kcal/mol and −9.34 kcal/mol in Asn499Asp and Asn499Lys mutants, respectively. The molecular docking represented that the in-

teraction energy of MFX in wild system was largest and mutant systems had smaller values.

The interaction properties of MFX were also characterised by MM-PBSA binding free energy during simulation.

**Table 1.** MM-PBSA binding free energy calculation result.

| System | VDW (kJ/mol) | ElecStat (kJ/mol) | Polar (kJ/mol) | Apolar (kJ/mol) | Total (kJ/mol) |
|---|---|---|---|---|---|
| Wild | −230.6 ± 3.0 | −339.9 ± 31.7 | 297.4 ± 15.3 | −17.7 ± 0.2 | −291.7 ± 21.1 |
| Asn499Asp | −210.5 ± 2.3 | −274.0 ± 30.7 | 337.9 ± 20.0 | −87.8 ± 1.5 | −233.9 ± 19.3 |
| Asn499Lys | −218.1 ± 2.9 | −146.0 ± 24.7 | 324.4 ± 16.3 | −18.6 ± 0.3 | −59.4 ± 13.8 |

VDW: Van der waals interaction, ElecStat: Electrostatic potential, Polar: Polar solvation energy, Apolar: Apolar solvation energy.

As shown in Table 1, the total binding free energy of MFX in wild system was largest as −291.7 kJ/mol and Asn499Asp and Asn499Lys mutants showed smaller binding free energies (*i.e.* Asn499Asp: −233.9 kJ/mol, Asn499Lys: −59.4 kJ/mol). In detail, Van der waals interaction energy and electrostatic potential in wild system were greater than mutant systems, and polar and apolar energy of wild system were less than mutant systems.

Also, residues interacting with MFX showed different contributions in binding free energy in different systems (Figure 5).

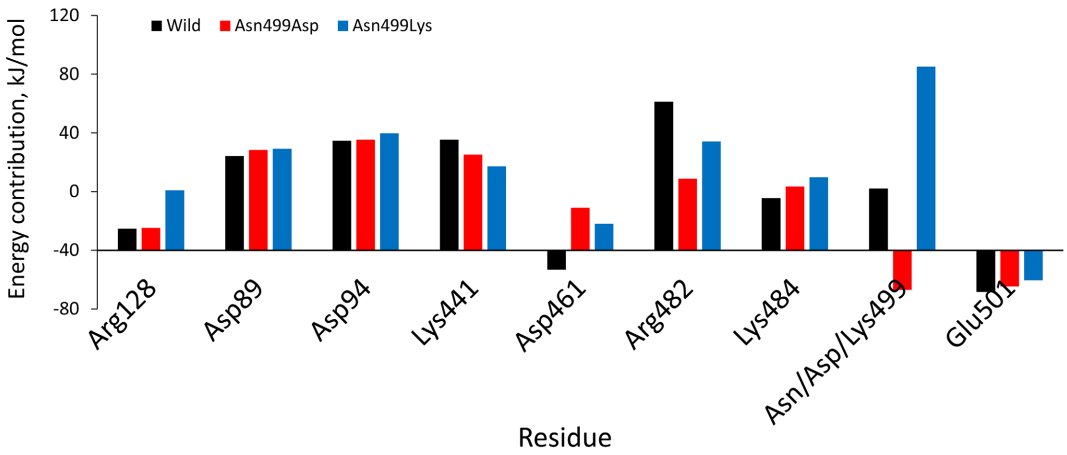


**Figure 5.** Contributions of MBS residues in MM-PBSA binding free energy.

Asp89, Asp94, Lys441, Lys484 and Glu501 had similar contributions in all systems but contribution of Arg128 in Asn499Lys mutant had increased compared to wild and Asn499Asp systems. Asp461 residue showed greater energy contribution in mutant systems, while Arg482 had opposite tendency. In particular, the residue of interest, Asn499, were completely different energy contributions in different systems. In wild system the contribution of binding free energy of Asn499 was almost zero but Asp499 made increase in binding energy between Asp499 and MFX and in reverse, Lys499 residue lowered the interaction energy of MFX, re-

ferring the impact of mutation of Asn499 residue in the MFX binding to gyrase.

### 3.4. Calculation of Distance between Tyr129 and DNA

During the breakage and reunion process, a transient covalent bond was formed between tyrosine of Gyrase A and DNA phosphate [26]. As the protein-DNA-ligand complex was stable, this covalent bond formation is stable. The distance between catalytic tyrosine at the 129th position of GyrA and DNA phosphate can reflect the stability of the cleaved complex.

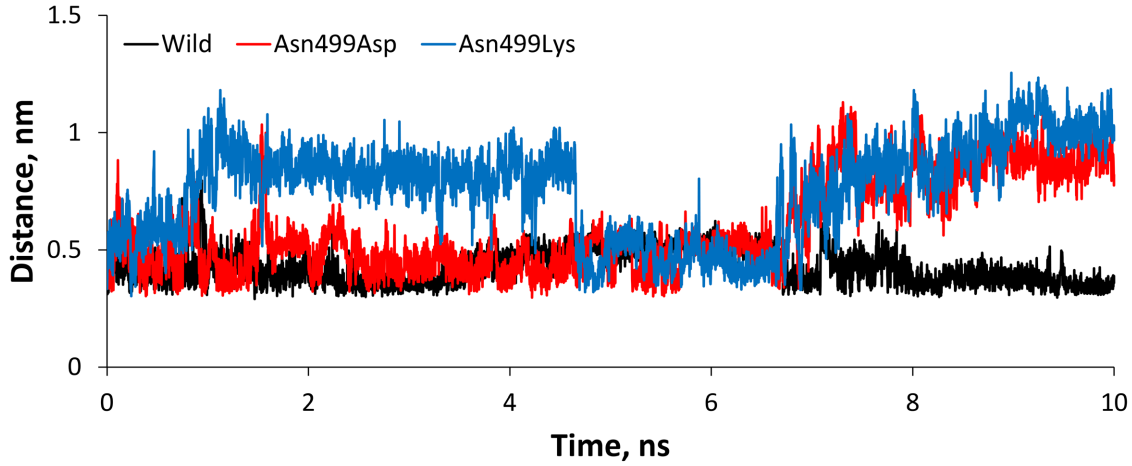


**Figure 6.** Distance between Tyr129 and DNA molecule during MD simulation.

As shown in **Figure 6**, the distances between Tyr129 and DNA in different systems were changed. In wild system, the distance was stable at ~0.4 nm during simulation but mutant systems showed fluctuating values, indicating change of interaction between Tyr129 and DNA molecule and resulting in unstable cleaved complex.

MD simulation result showed the unstable cleaved complex in mutant systems, indicating the decrease in the gyrase-inhibiting activity of MFX. Also, the distance of Tyr129 and DNA molecule were fluctuating, not stable in mutant systems compared to wild system, resulting in the adverse impact on the stability of cleaved complex.

## 4. Conclusions

The present study was designed to determine the effect of mutation Asn499Asp and Asn499Lys of gyrase on the moxifloxacin resistance. No research which mentioned the resistance mechanism of this mutation site, Asn499 was found. In the current study, the structural and interaction profiles of gyrase-DNA-MFX complex were compared in wild and mutants. MD simulation result showed the unstable cleaved complex in mutant systems, indicating the decrease in the gyrase-inhibiting activity of MFX. Molecular docking study demonstrated that the interaction energy of MFX and mutant gyrase decreased than those in wild system.

Also, MM-PBSA binding free energy calculation showed the decrease energy in mutant systems. These findings provided direct evidence for the unstable binding of MFX in mutants. Specifically, the interaction energy of MFX and Asn499 residue were changed, resulting in the impact to the overall binding mode of MFX. Again, in wild gyrase, MFX did not interact with Asn499 residue but in mutant gyrases MFX could interact with this residue.

In conclusion, the MFX resistance conferred by gyrase mutated in Asn499 residue was caused by the structural instability of cleaved complex and corresponding change of MBS, resulting in the alteration of binding mode of MFX and MBS. These findings have important implications for developing new drugs for moxifloxacin-resistant patients.

## Acknowledgements

The authors acknowledge Tim R. Blower for providing gyrase-fluoroquinolone cleaved complex. We also thank all programmers for providing GROMACS package.

## Conflicts of Interest

The authors declare that they have no competing interests.

## References

[1] WHO (2021) Global Tuberculosis Report 2021. World Health Organization.

[2] Blumberg, H.M., Burman, W.J., Chaisson, R.E., Daley, C.L., Etkind, S.C., *et al.* (2003) American Thoracic Society, Centers for Disease Control and Prevention and Infectious Diseases Society of America, Treatment of tuberculosis. *American Journal of Respiratory and Critical Care Medicine*, **167**, 603-662.

[3] Pranger, A.D., van der Werf, T.S., Kosterink, J.G.W. and Alffenaar, J.W.C. (2019) The Role of Fluoroquinolones in the Treatment of Tuberculosis in 2019. *Drugs*, **79**, 161-171. https://doi.org/10.1007/s40265-018-1043-y

[4] Khisimuzi, M. and Ma, Z.K. (2007) *Mycobacterium tuberculosis* DNA Gyrase as a Target for Drug Discovery. *Infectious Disorders—Drug Targets*, **7**, 159-168. https://doi.org/10.2174/187152607781001763

[5] Shantanu, K. and John Innes, C. (2010) Development of *Mycobacterium tuberculosis* DNA Gyrase as a Target for Antibacterial Chemotherapy. Degree of Doctor of Philosophy at the University of East Anglia.

[6] Peter, H. and Andrew, T. (2010) The Ternary Gyrase-DNA-Quinolone Complex: From Molecular Modelling to Understanding Quinolone Action and Resistance. Institute for Pharmacy.

[7] Maruri, F., Sterling, T.R., Kaiga, A.W., Blackman, A., van der Heijden, Y.F., Mayer, C., *et al.* (2012) A Systematic Review of Gyrase Mutations Associated with Fluoroquinolone-Resistant *Mycobacterium tuberculosis* and a Proposed Gyrase Numbering System. *Journal of Antimicrobial Chemotherapy*, **67**, 819-831. https://doi.org/10.1093/jac/dkr566

[8] Blower, T.R., Williamson, B.H., Kerns, R.J. and Berger, J.M. (2016) Crystal Structure and Stability of Gyrase-Fluoroquinolone Cleaved Complexes from *Mycobacterium tuberculosis*. *Proceedings of the National Academy of Sciences*, **113**, 1706-1713.

https://doi.org/10.1073/pnas.1525047113

[9] Hooper, C.D. and Rubinstein, E. (2003) Quinolone Antimicrobial Agents. ASM Press.

[10] Aubry, A., Veziris, N., Cambau, E., Truffot-Pernot, C., Jarlier, V. and Fisher, L.M. (2006) Novel Gyrase Mutations in Quinolone-Resistant and Hypersusceptible Clinical Isolates of *Mycobacterium tuberculosis*: Functional Analysis of Mutant Enzymes. *Antimicrobial Agents and Chemotherapy*, **50**, 104-112.

[11] Von Groll, A., Martin, A., Jureen, P., Hoffner, S., Vandamme, P., Portaels, F., *et al*. (2009) Fluoroquinolone Resistance in *Mycobacterium tuberculosis* and Mutations in gyrA and gyrB. *Antimicrobial Agents and Chemotherapy*, **53**, 4498-4500. https://doi.org/10.1128/aac.00287-09

[12] An, D.D., Hong Duyen, N.T., Lan, N.T.N., Hoa, D.V., Ha, D.T.M., Kiet, V.S., *et al*. (2009) Beijing Genotype of *Mycobacterium tuberculosis* Is Significantly Associated with High-Level Fluoroquinolone Resistance in Vietnam. *Antimicrobial Agents and Chemotherapy*, **53**, 4835-4839. https://doi.org/10.1128/aac.00541-09

[13] Malik, S., Willby, M., Sikes, D., Tsodikov, O.V. and Posey, J.E. (2012) New Insights into Fluoroquinolone Resistance in *Mycobacterium tuberculosis*: Functional Genetic Analysis of gyrA and gyrB Mutations. *PLOS ONE*, **7**, e39754. https://doi.org/10.1371/journal.pone.0039754

[14] Abraham, M.J., Murtola, T., Schulz, R., Páll, S., Smith, J.C., Hess, B., *et al*. (2015) GROMACS: High Performance Molecular Simulations through Multi-Level Parallelism from Laptops to Supercomputers. *SoftwareX*, **1**, 19-25. https://doi.org/10.1016/j.softx.2015.06.001

[15] Oostenbrink, C., Villa, A., Mark, A.E. and Van Gunsteren, W.F. (2004) A Biomolecular Force Field Based on the Free Enthalpy of Hydration and Solvation: The GROMOS Force-Field Parameter Sets 53A5 and 53A6. *Journal of Computational Chemistry*, **25**, 1656-1676. https://doi.org/10.1002/jcc.20090

[16] Schüttelkopf, A.W. and van Aalten, D.M.F. (2004) PRODRG: A Tool for High-Throughput Crystallography of Protein-Ligand Complexes. *Acta Crystallographica Section D Biological Crystallography*, **60**, 1355-1363. https://doi.org/10.1107/s0907444904011679

[17] Berendsen, H.J.C., Postma, J.P.M., van Gunsteren, W.F., DiNola, A. and Haak, J.R. (1984) Molecular Dynamics with Coupling to an External Bath. *The Journal of Chemical Physics*, **81**, 3684-3690. https://doi.org/10.1063/1.448118

[18] Parrinello, M. and Rahman, A. (1981) Polymorphic Transitions in Single Crystals: A New Molecular Dynamics Method. *Journal of Applied Physics*, **52**, 7182-7190. https://doi.org/10.1063/1.328693

[19] Essmann, U., Perera, L., Berkowitz, M.L., Darden, T., Lee, H. and Pedersen, L.G. (1995) A Smooth Particle Mesh Ewald Method. *The Journal of Chemical Physics*, **103**, 8577-8593. https://doi.org/10.1063/1.470117

[20] Hess, B., Bekker, H., Berendsen, H.J.C. and Fraaije, J.G.E.M. (1997) LINCS: A Linear Constraint Solver for Molecular Simulations. *Journal of Computational Chemistry*, **18**, 1463-1472. https://doi.org/10.1002/(sici)1096-987x(199709)18:12<1463::aid-jcc4>3.0.co;2-h

[21] Hou, X.B., Du, J.T., Zhang, J., Du, L.P., Fang, H. and Li, M.Y. (2013) How to Improve Docking Accuracy of AutoDock4.2: A Case Study Using Different Electrostatic Potentials. *Journal of Chemical Information and Modeling*, **53**, 188-200. https://doi.org/10.1021/ci300417y

[22] Wang, X.M., Wu, S.S., Xu, D.G., Xie, D.G. and Guo, H. (2011) Inhibitor and Substrate

Binding by Angiotensin-converting Enzyme: Quantum Mechanical/Molecular Mechanical Molecular Dynamics Studies. *Journal of Chemical Information and Modeling*, **51**, 1074-1082. https://doi.org/10.1021/ci200083f

[23] Vorontsov, I.I. and Miyashita, O. (2011) Crystal Molecular Dynamics Simulations to Speed up MM/PB(GB)SA Evaluation of Binding Free Energies of Di-Mannose Deoxy Analogs with P51G-m4-Cyanovirin-N. *Journal of Computational Chemistry*, **32**, 1043-1053. https://doi.org/10.1002/jcc.21683

[24] Disratthakit, A., Prammananan, T., Tribuddharat, C., Thaipisuttikul, I., Doi, N., Leechawengwongs, M., *et al*. (2016) Role of gyrB Mutations in Pre-Extensively and Extensively Drug-Resistant Tuberculosis in Thai Clinical Isolates. *Antimicrobial Agents and Chemotherapy*, **60**, 5189-5197. https://doi.org/10.1128/aac.00539-16

[25] Pandey, B., Grover, S., Tyagi, C., Goyal, S., Jamal, S., Singh, A., *et al*. (2017) Double Mutants in DNA Gyrase Lead to Ofloxacin Resistance in *Mycobacterium tuberculosis*. *Journal of Cellular Biochemistry*, **118**, 2950-2957. https://doi.org/10.1002/jcb.25954

[26] Piton, J., Petrella, S., Delarue, M., André-Leroux, G., Jarlier, V., Aubry, A., *et al*. (2010) Structural Insights into the Quinolone Resistance Mechanism of *Mycobacterium tuberculosis* DNA Gyrase. *PLOS ONE*, **5**, e12245. https://doi.org/10.1371/journal.pone.0012245